UCRL-JC-128363
PREPRINT

Modeling of laser-induced surface cracks in silica at 355 nm

M. D. Feit, J. Campbell, D. Faux, F. Y. Génin, M. R. Kozlowski,
A.M. Rubenchik, R. Riddle, A. Salleo, and J. Yoshiyama,

This paper was prepared for and presented at the
XXIX Annual Syposium on Optical Materials for High Power Lasers
Boulder, Colorado
October 6-8, 1997

December 1997

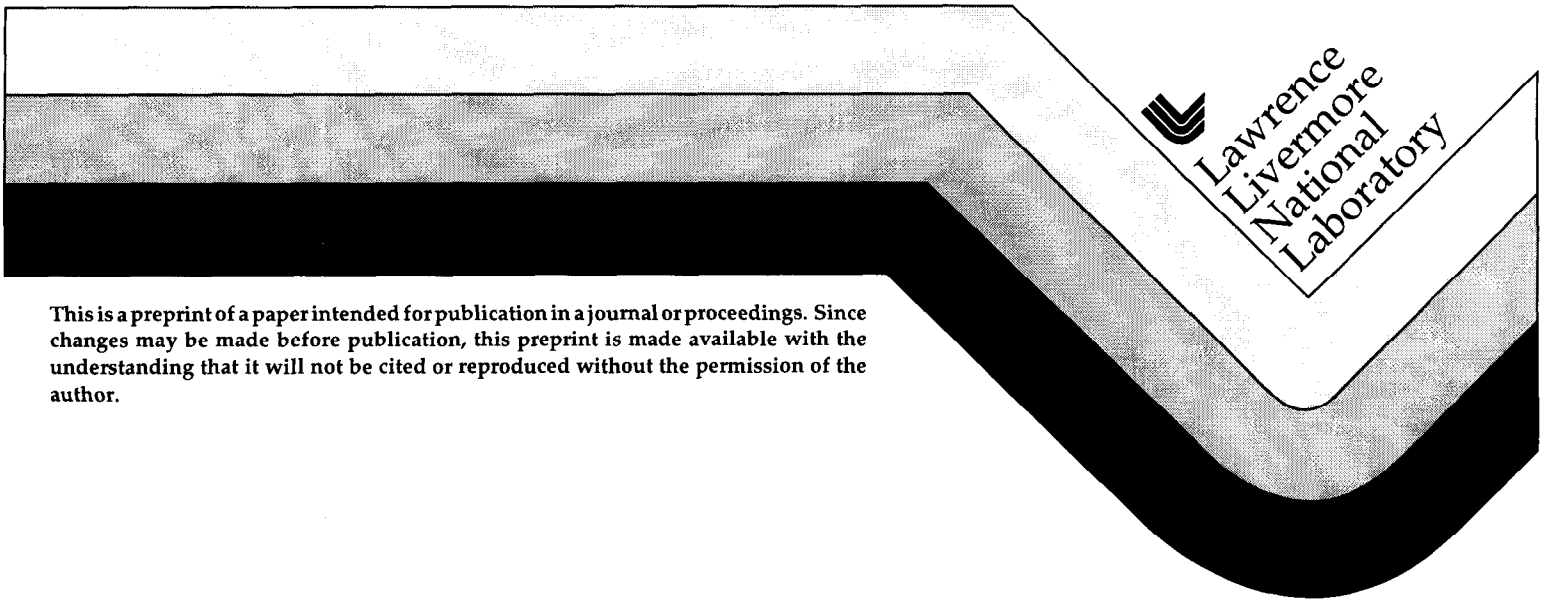

Modeling of laser-induced surface cracks in silica at 355 nm *

M. D. Feit, J. Campbell, D. Faux, F. Y. Génin, M. R. Kozlowski,
A.M. Rubenchik, R. Riddle, A. Salleo, and J. Yoshiyama,

Lawrence Livermore National Laboratory,
mail stop L-439
Livermore, California 94550, U.S.A.
feit1@llnl.gov

Summary

Starting from the absorption of laser energy at a subsurface nanoparticle in fused silica, we simulate the consequent buildup of stresses and resulting mechanical material damage . The simulation indicates the formation of micropits with size comparable to a wavelength, similar to experimental observation. Possible mechanisms for enhanced local light absorbtion are discussed.

Keywords: nanoparticles, laser absorption, heating, brittle fracture

*Work performed under the auspices of the U. S. Department of Energy by Lawrence Livermore National Laboratory under Contract No. W-7405-ENG-48.

I. Introduction

The NIF final optics will operate at wavelength of 355 nm (3ω or third harmonic of 1 μm light). Optical damage at 3ω is a more severe problem than for first harmonic radiation. Damage is typically initiated in a nearsurface layer, usually on the exit side of the opical element. Experiments indicate that damage is initiated at subwavelength sites. Local heating of nanoparicles can result in material crushing due to thermal induced stress. Also thermal explosion in which the absorbing region grows in size with heating can play a role.

Experimental observation shows that micropit damage spots appear near the laser damage threshold, particularly on the exit side of fused silica samples (see. Fig.1). All micropits have comparable sizes, with depth comparable to the width. It is noticeable that pits tend to be elongated, and cracks open preferentially, normal to the electric field polarization direction.

It is natural to think that such pits are initiated by subwavelength particulate absorbers in the subsurface layer. Such an absorber might be a small contaminant particle, for example due to the polishing process. To be specific, we consider ceria particles below, but later we will discuss other possibilities. Heating the material around the absorber can result in further absorbtion increase, thermal explosion and material ejection forming the pits.

II. Linear absorption by small particles

Consider a spherical particle, much smaller than an optical wavelength, embedded in a transparent medium with refractive index n. Light energy is absorbed at the rate $Q = \sigma I(t)$, with σ being the absorption cross section. It can be shown[1] that the absorption cross section for a small particle of radius a is given to good approximation by [see refs 1,2]

$$\sigma=\frac{12\pi\, n\omega\, a^3}{c}\,\mathrm{Im}\left[-\frac{n^2}{\varepsilon+2\,n^2}-\frac{1}{6}+\frac{1}{2(ka)^2}-\frac{Cot(\,ka)}{2\,ka}\right] \qquad (1)$$

where ε is the complex dielectric coefficient of the inclusion, k_0 is the optical wavenumber in the vacuum and $k=\sqrt{\varepsilon}\, k_0$ is the wavenumber in the inclusion, n is the refractive index for the matrix (1.5 for glass), and "small particle" means $k_0 a \ll 1$.

The fraction of light incident on the geometric cross section which is absorbed is given by $\alpha = \sigma/\pi a^2$. Starting from a very small radius a, α will initially grow faster than linearly with a, and then, if the dielectric coefficient is of large magnitude, tend to saturate[1]

$$\alpha = 6n/\sqrt{\varepsilon} \text{ if } \omega\varepsilon a/c \gg 1 \qquad (2)$$

Because of diffraction, this absorption fraction can be larger than unity.

The size of the absorber is typically much smaller than a thermal diffusion length. The temperature in the surrounding material can be treated as stationary, ie

$$T(r) = T_0\left(\frac{a}{r}\right) \quad for \quad a < r < \sqrt{4Dt}$$

$$where \quad T_0 = \frac{\alpha I a}{4K} \qquad (3)$$

where K is the thermal conductivity and D the thermal diffusivity.

In Fig. 2 we present the peak temperature T_0 for a ceria particle with refractive index n=2 + 0.2 i. The light intensity was assumed to be 3 GW/cm^2 and the pulse duration was taken as 3 ns. The thermal conductivity was taken as 0.014 W/cm K .

Here ka=0.5 corresponds to a ceria particle with radius about 28 nm. The peak temperature grows as the square of particle size for small particles. This result demonstrates why the NIF third harmonic light is more dangerous than the fundamental. The absorption efficiency depends on the particle size measured in wavelengths so is effectively three times as large at the third harmonic. In addition, the dielectric constant of most materials is larger in the infrared than in the UV which causes additional absorption.

III. Thermoelastic stress

When the temperature distribution is known, the thermoelastic stresses can be calculated[3]. For example, Fig.(3) shows the xx component of stress for a spherical ceria particle embedded in fused silica. The peak temperature was assumed to be 1000K and the coordinates are given in terms of the particle radius. Notice that the radial stress (equatorial in the figure) is compressive while the tangential or hoop stress (at the poles) is tensile.

For an infinite medium, the stress distribution is symmetric as shown. For a near surface particle, the presence of the free surface modifies the distribution and material failure most likely occurs initially around the equator of the particle (the "pole" is directed toward the surface).

IV. Glass Damage

We used the DYNA2D code to model the damage to fused silica due to heating of a near surface subwavelength ceria particle. A tensor damage model was used to describe the mechanical damage of brittle material. For low loading, elastic waves can propagate. At higher loads, limited plasticity and tensile and compressive failure can occur. The fact that material strength is larger for loads applied only a short time is taken into account. A polynomial equation of state accounting for the energy dependence of the bulk modulus and Gruneisen coefficient was used for the fused silica. Parameters in the model were determined from experiments on high velocity projectile impacts on glass.

Again we consider a ceria particle embedded in glass. It was assumed that the glass outside the particle is nonabsorbing. The ceria particle was described with the same type of damage model as the glass, but with different parameters.

In the runs presented below we consider 100 nm radius particles at distances of 300 nm and 150 nm from the surface. Energy was deposited at a constant rate for 3 nsec which corresponds to a laser fluence 10 J/cm^2 . Fig.4 shows the damage distribution in ceria and glass for particle placed 300 nm under surface at 1,2 and 3 nsec respectively. The figure indicates the amount of damaged material. Because thermal expansion in ceria is much larger than that of fused silica(130×10^{-7}/K vs 7×10^{-7} /K), thermal expansion generates the initial stresses and damage in the surrounding material. Simultaneously, the shock reaches the free surface and reflects back generating tensile stresses which easily damage the material. As noted above, because of the free surface, fracture propagates from the equator toward the free surface as additional

material fails as stresses are redistributed. The damaged region forms a characteristic conical shape. At the closest and furtherest parts of the region, the particle stresses are mainly compressive and initially don't damage the material. Later increases in pressure and arrival of the reflected wave crush most of the material within the cone. All mechanical resistance to shear is destroyed within the cone. The crushed material is finally ejected, forming a conical pit similar to that observed in experiments. The velocity of ejection is not high, 150-200 m/sec . It takes a comparitively long time to evacuate the pits. If the completely damaged material is taken as the eventual pit boundary, the estimated pit diameter is about 800 nm and the depth about 400 nm.

Fig. 5. shows the extent of damage for a particle barried shallower, at 150 nm below the surface at 1.8 nsec. The effect of the free surface is more pronounced; the damage starts occurs less symmetrically. The glass experiences pressure of 25 kbar prior to damage. The conical fracture appears with the cone narrower than in the deeper particle case. The surface damage has grown down and converged with particle. Crushed material fills the cone and ejection of material is already started at a velocity 2 times larger than in the first case. The depth of the crater is about 250 nm and the width about 500 nm. Pit depth is not very sensitive to the distance from the surface, in both case it is 50-100 nm below the particle boundary; pit width is much wider for a deeply barried particle. The ejected (crushed) zone includes the particle all contaminants are ejected.

This modeling didn't take into account thermal explosion, ie. growth of absorption with contaminant heating. We will estimate this effect in the next section.

V. Thermal Explosion

When the temperature around the inclusion reaches a critical value, a thermal explosion takes place[5,6]. This involves the rapid expansion of the heated region into the glass which is then ionized. It occurs because the plasma produced by the initially absorbed light radiates UV which is strongly absorbed in the matrix resulting in heating and an increase in the absorption coefficient of the glass. The situation is very similar to laser supported ionization waves [6,7], the main difference being that absorption occurs in a volume instead of just at a front.

In the following, we assume the Drude model for the dielectric coefficient of the plasma:

$$\varepsilon = 1 - \frac{n_e}{n_c\left(1+\frac{i\nu}{\omega}\right)} \approx -\frac{n_e}{n_c}\left(1-\frac{i\nu}{\omega}\right) \tag{4}$$

where n_e is the electron density, n_c the critical density and ν is the collision frequency.

Consider the situation with plasma density larger than critical, and electron scattering rate smaller than the light frequency. We assume that radiation is trapped, and all absorbed energy is spent to ionize the material. The rate of growth of the plasma ball can be estimated from energy balance:

$$nI_0 4\pi a^2 \frac{da}{dt} = \sigma I(t) \tag{5}$$

If one uses only the first term in Eq(1) for the absorption cross section, the radius of the ball grows exponentially: $a = a(0)\exp G$, where the growth factor G is given by

$$G = 10\frac{F\omega}{nI_0 c}\,\mathrm{Im}\frac{1}{\varepsilon+2} \tag{6}$$

For absorption at 3ω, and a solid state density of about ten times critical, ionization potential of 10 eV, fluence F of $10 J/cm^2$, and scattering rate 0.5 of the optical frequency, the growth factor G is about 10. Taking into account the growth of absorptivity with increase of radius, we can say that if plasma formation starts, the plasma ball will rapidly grow to a size for which ka>1. Using Eq(2) for the absorption cross-section, we have

$$a(t) = 3.5\,\mathrm{Re}\frac{1}{\sqrt{\varepsilon}}\frac{\int_{-\infty}^{t} I(t)dt}{nI_0} \tag{7}$$

The plasma sphere radius at the end of the pulse is seen to be

$$a = 3.5\,\mathrm{Re}\frac{1}{\sqrt{\varepsilon}}\frac{F}{nI_0} \tag{8}$$

where F is the fluence and I_0 the ionization energy.

For the parameters used above, this radius a is about 500 nanometers. The rate of plasma ball growth drops dramatically in this regime. When the size of the plasma ball becomes comparable or larger than the optical wavelength, Eq.(1) is no longer reliable. It appears that these considerations don't change the results of the previous section very much. In any case, because of crushed material and the nearby free surface, some additional absorption most likely leads to higher velocity of ejecta rather than to removal of additional material.

VI. Conclusions

It was demonstrated that even small absorbers can be heated up to very high temperature by UV radiation in the NIF operation range. The subsequent thermal stresses and possible thermal explosion results in creation of high pressures and glass damage. Similations indicate a conical shaped micropit damage region with width and depth comparable to the laser wavelength. These micropits serve as "seeds" for subsequent growth of damage with further laser shots. We modeled here an absorbing contaminant particle, but the initiating absorption might also be caused by absorption at color centers or by 3ω multiphoton absorption near cracks where intensification can occur and the bandgap can be locally reduced.

Once the pit begins to form, the polarization dependence of subsequent crack growth can be understood from the different boundary conditions at vertical pit or crack walls for S or P polarization.

References

1. L. D. Landau and E.M. Lifshitz, "*Electrodynamics of continuous media*", Pergammon Press (New York, 1960).
2. H. van de Hulst, " *Light scattering by small particles*", Dover Publications. (New York, 1981)
3. A.P. Boresi , "*Elasticity in Engineering Mechanics*", Prentice Hall,(New Jersey, 1965)
4. R.G. Whirley, B.E. Engelmann, and J.O. Hallquist, "DYNA2D A Nonlinear, Explicit, Two-Dimensional Finite Element Code For Solid Mechanics ", LLNL report UCRL-MA-110630 (1992)
5. M.F. Koldunov, A.A. Manenkov, I.L. Pokotilo, Sov. J. Quant. Electr. **18**, 345 (1988)
6. S. I. Anisimov and V.A. Khokhlov, "*Instabilities in laser-matter interaction*", CRC Press, (Boca Raton, Florida, 1995)
7. M. von Allmen and A. Blatter, "*Laser beam interactions with materials*", Springer (Berlin, 1994)

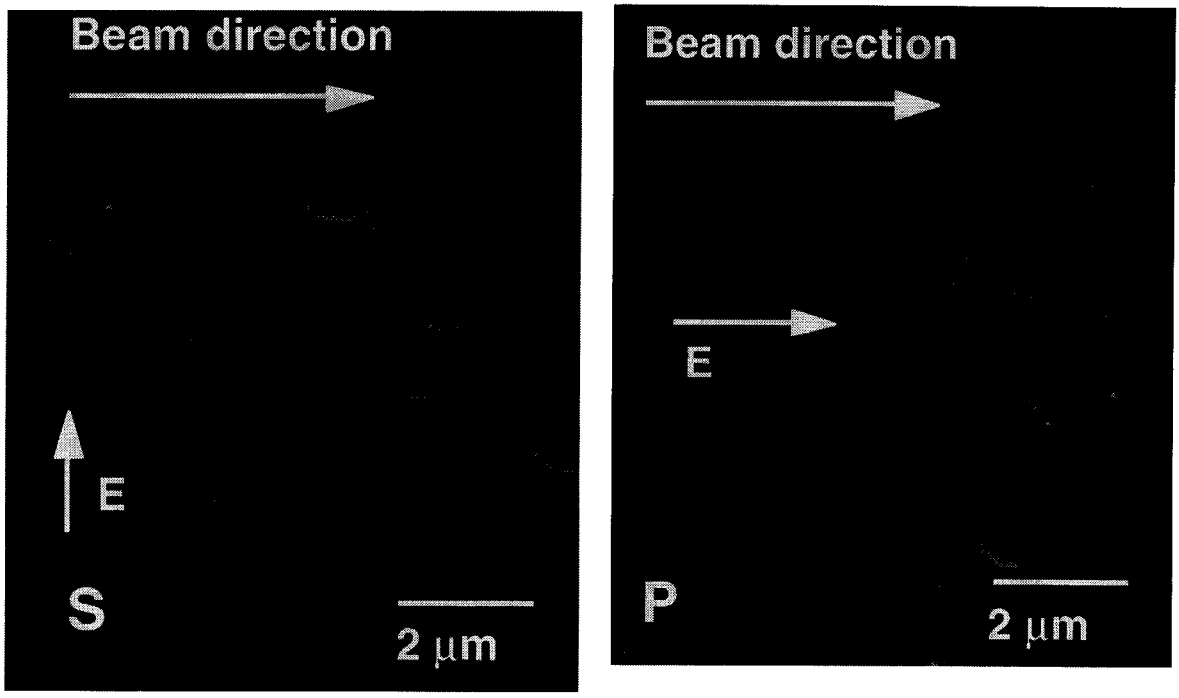

Fig. 1: Micropit laser induced damage observed on initially pit free fused silica surface shows characteristic subwavength size and orientation with respect to polarization of laser electric field.

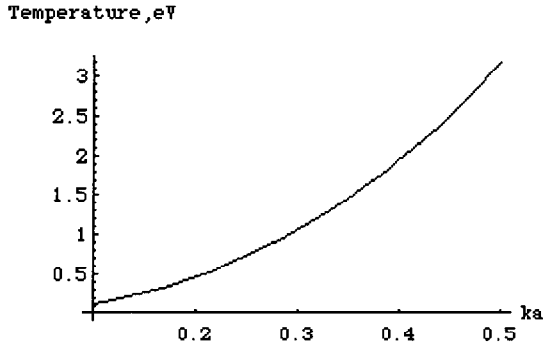

Fig. 2 . Peak temperature increase at a ceria particle of radius a embedded in fused silica. Laser fluence was 9 J/cm^2 at 3ω.

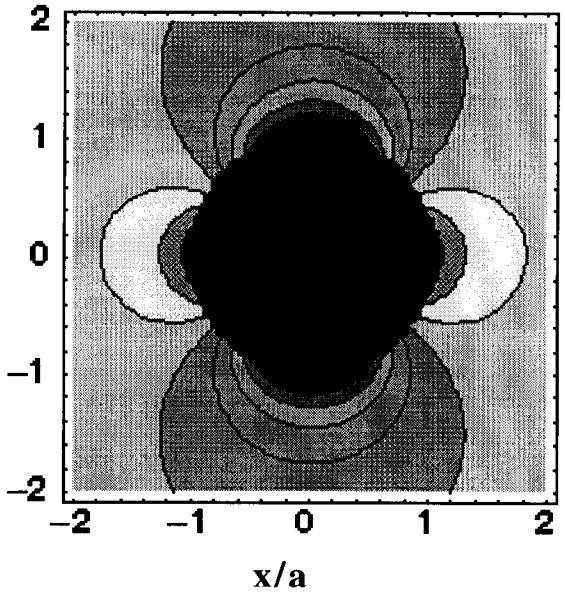

Fig. 3 Variation of xx component of stress near embedded ceria particle in silica. Peak temperature is 1000K and drops off as 1/r outside particle. Radial stress is compressive and hoop stress in tensile at interface.

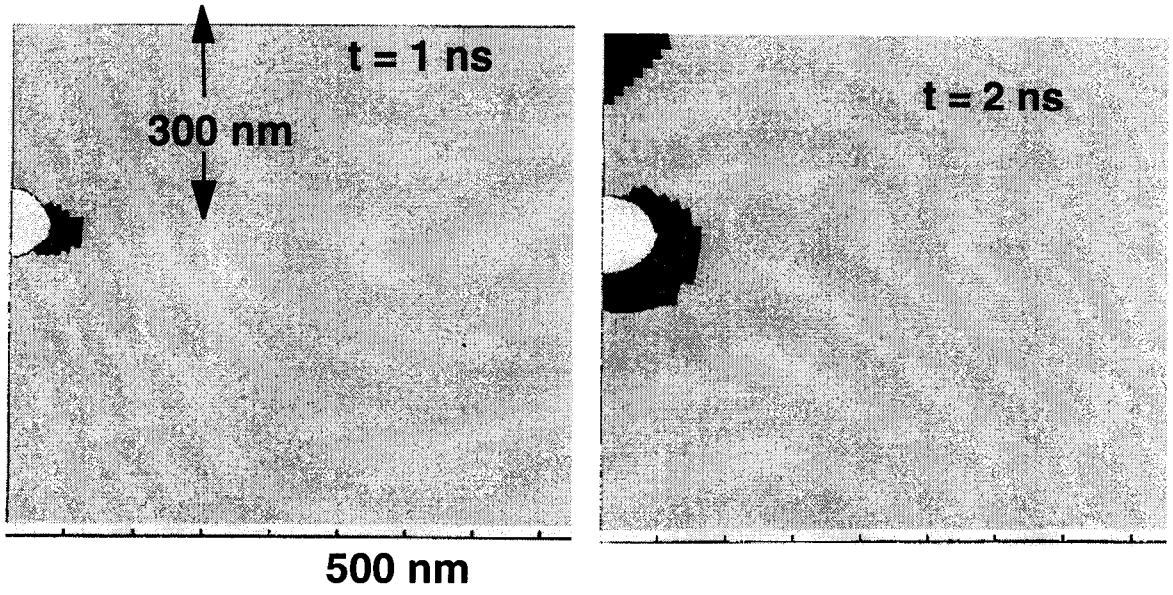

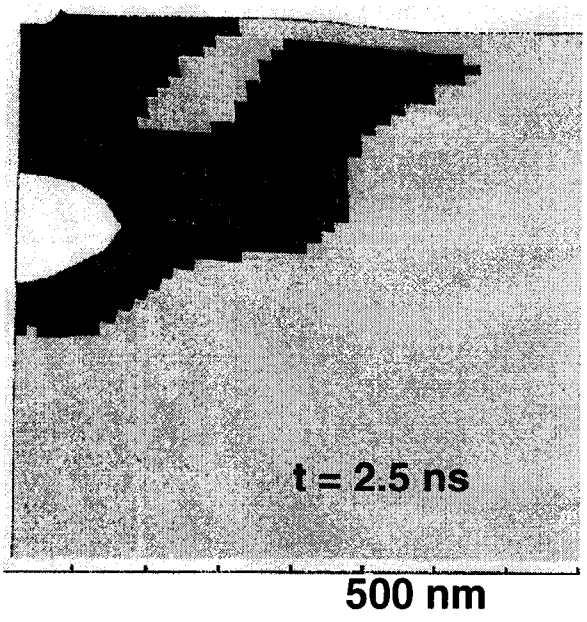

Fig. 4: Growth of material damage in fused silica due to buried 100 nm ceria particle 300 nm below the surface. Damage initiates near the particle equator and grows to the surface to form a conical region.a) after 1 ns irradiation, (b) 2 ns, (c) 2.5 ns . The material inside the conical region is eventually completely crused and ejected.

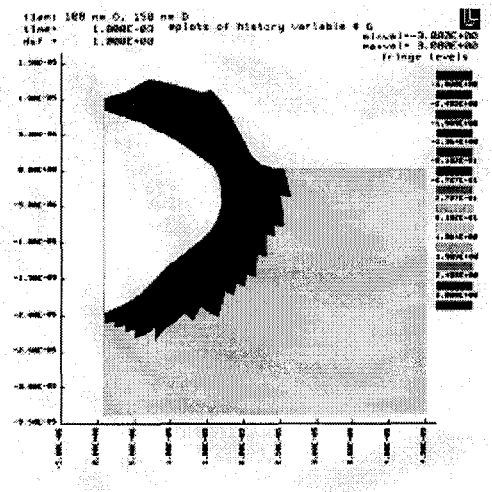

Fig. 5: Growth of material damage in fused silica due to buried 100 nm ceria particle 150 nm below the surface at time 1.8 nsec. Material is more distorted than for deeper particle and has already begun to be ejected..

Technical Information Department • **Lawrence Livermore National Laboratory**
University of California • Livermore, California 94551